ORIENTAL JOURNAL OF CHEMISTRY
An International Open Access, Peer Reviewed Research Journal
www.orientjchem.org
ISSN: 0970-020 X
CODEN: OJCHEG
2025, Vol. 41, No.(5):
Pg. 1610-1618

Synthesis and Characterization of Novel Potassium Ethane-1,2-diylbis((2-bromobenzyl)carbamodithioate) Complexes, Along with an Investigation of their Biological Activity

AEED S. AL-FAHDAWI[1]* and HANAN KHAMEES KHALAF AL-DULYMI[2]

[1]Department of Chemistry, College of Education for Women, University of Anbar, Iraq.
[2]Department of Chemistry, College of Science, University of Anbar, Iraq.
*Corrsponding author E-mail: edw.aeedchemistry@uoanbar.edu.iq,
Hanan.khamees@uoanbar.edu.iq

http://dx.doi.org/10.13005/ojc/410516

(Received: September 10, 2025; Accepted: October 16, 2025)

ABSTRACT

In this study, the synthesized ligand and its complexes demonstrated notable antibacterial activity against several pathogenic bacteria. The Spectroscopic and analytical characterisation of a group of metallic complexes(II) belonging to the ligand dithiocarbamate were prepared, the ligand was prepared from three stepes. Follow: I. preparation of Schiff base by reaction Ethelinediamin with Bromobenzaldehyde. II. Reaction the product's Schiff base with Soduimborohydrate to yield Secondary Amin. III. Theproduct secondary amin reacted with carbondisulfide to producted ligand, which reacted with metal ion to yield dithiocarbamate complexes. The spatial shape around the ionic centers of the complexes was determined using a number of physic-chemical and spectroscopic techniques, including. UV-Vis, ^{1}H-NMR, FTIR, mass spectrometers, melting points, and conductivity. This analytical and spectroscopic data showed that the MnII, FeII, CoII, NiII, CuII, and ZnII ions had a tetrahedral shape and square planar geometry with Ni(II) complexes. The antibacterial activity of ligands and complexes was evaluated with two types of bacteria: *Staphylococcus aureus (Gram-positive)* and *Escherichia coli (Gram-negative)*. Zone of inhibition assays further supported these findings showing clear inhibition Zone of up to 15mm around the complexes. May be its disrupt bacterial cell membrane integrity and inhibit essential complexesas effective antibacterial agent.

Keyworlds: Dithiocarbamate complexes, Antibacterial, Macrocyclic Inorganic chemistry, Complexes Characterization, Octahedral and Tetrahedral.

INTRODUCTION

The journey for unused antibacterial specialists has ended up progressively basic in light of rising antimicrobial resistance[1]. This ponder centers on the union and characterization of a novel ligand, potassium ethane-1,2-diylbis((2-bromobenzyl) carbamodithioate) complexes. These complexes are balanced to improve our understanding of metal-ligand intuitive whereas illustrating potential helpful applications[2]. Characterization of the synthesized complexes will be conducted utilizing different

methods, counting infrared spectroscopy, and atomic attractive reverberation. These strategies will offer assistance explain the auxiliary highlights and affirm the effective arrangement of the complexes[3,4]. Ligands with interesting auxiliary properties can altogether impact the natural exercises of metal complexes. The joining of metal ion with dithiocarbamate ligand is especially vital; it is known for its differing pharmacological properties, counting antimicrobial impacts. By investigating the interaction between this ligand and metal ions, we point to create complexes that display upgraded steadiness and bioactivity[5,6]. By giving a union, characterization, and organic assessment of these complexes, this inquire about points to contribute to the progressing explore for successful antimicrobial operators, advertising a establishment for future advancements in restorative chemistry.[7,8] The knowledge into the natural assessment of these novel complexes, this research points to contribute to the progressing rummage around for compelling antimicrobial operators, advertising a establishment for future advancements in therapeutic chemistry[9,10].

MATERIAL AND EXPRIMENTAL

Materials

2-Bromobenzaldehyde (BrC_6H_4CHO), Ethylenediamine($C_2H_8N_2$), potassium hydroxide (KOH), methanol (CH_3OH), carbon disulphide (CS_2), and dimethyl sulfoxide (DMSO) were bought from B.D.H, Merck, Fluke, and Sigma-Aldrich, and used without additional purification. Solvents were purified by distillation.

Synthesis of the Schiff base

Preparation of the Schiff-base (N^1Z, N^2E)-N^1,N^2-bis(2-bromobenzylidene)ethane-1,2-diamine was prepared by dissolving (3.07 g,16.6 mmol) of 2-Bromobenzaldehyde in (10 mL) of methanol and (3-4) drops of HBr, then (0.50 g, 8.31 mmol) of Ethylenediamine was added to the solution. Then the mixture was left for the reflux process for (3) h at a temperature of (76-78^{0}C). After the reaction was completed, the mixture was left to cool and filtered, then the solvent was evaporated under vacuum pressure, giving a white precipitate with a weight of 2.94 g, (89.9%), m.p. = 95-97^{0}C.

Preparation of secondary amine

The compound Schiff base was prepared dissolved (0.42 g, 1.06 mmol) from a Schiff base. In 40 mL (1:1) of the dichloromethane/methanol mixture, was added (0.24 g, 6.31 mmol) from $NaBH_4$ to the solution, in an ice bath, leave the mixture to stir For a period of (12 h), the organic layer was separated by adding (200 mL) water to the additive solution dichloromethane and the organic layer was washed with water four times (50x4 mL) and then dried With $MgCO_3$, After the filtering and removing of the solvent by evaporation, the result is washed with diethyl ether. The product yellow solid.Yield: 0.30 g (71.4%). m.p. = 87-89^{o}C.

Synthesis of ligand [L]

The ligand Potassium ethan-1,2-diylbis((2-bromobenzyl)carbamodithioate was prepared by dissolving (0.50 g,1.25 mmol) of the aforementioned secondary amine in (20 mL) of methanol, and adding to it (0.14 g, 2.5 mmol) dissolved in (5 mL) of methanol, with continuous stirring for 15 minutes after which the solution was cooled in an ice bath to add (0.18 g, 2.48 mmol) of CS2 was left to stir continuously for(2-3) h to give the precipitate dithiocarbamate salt formed after filtering and washing with methanol and ether and then drying it under vacuum pressure to give a white precipitate by weight 0.63 g (90%), m.p. = 100-102^{o}C .

General synthesis of macrocyclic-based complexes

The complexes were prepared from the reaction of one mole of the potassium dithiocarbamate (K-DTC) salt against one mole of the mineral salt as a central ion to have the ratio (1:1), as the metals used to prepare the cyclic complexes are Mn(II), Fe(II), Co(II), Cu(II) , Ni(II), and Zn(II). The mixture containing the ligand salt and the metal and their solvents are stirred for 24 h, and distilled water is added if necessary to complete the sedimentation. We obtain the precipitate by filtering, washing it with solvent, and drying it to give complexes of different colors according to the type of metal to give the ring complex.

Determination of bacteriological activity

The biological activity of the ligand and selected complexes, $[Mn(L)]_2$, $[Fe(L)]_2$, $[Co(L)]_2$, $[Ni(L)]_2$, $[Cu(L)]_2$, and $[Zn\ (L)]_2$, was studied on two different types of bacteria.

Some chemicals were tested and a solvent (DMSO) was employed. 50, 100, and 150 mg/mL. The 50 and 100 mg/mL concentrations were chosen

for the biological action. The bioactivities were examined by agar well diffusion. The wells were dug in the media with the help of a sterile metallic borer with centers of at least 24 mm. The concentration of (50 and 100) mg/mL in DMSO was applied to each well. The plates were incubated at 37°C for 24 hours. Zones indicating complete inhibition were used to determine the activity (mm). Increasing the width of the inhibition signifies an increase in the biological efficacy of the produced compounds compared to antibiotics' (Ghoto, Khuhawar and Jahangir, 2019).

Phyasical Mesuerment

An Electro-Thermal Stuart melting point apparatus was used to determine the melting points of compounds. On a Shimadzu and Bruker (FTIR)–8400S spectrophotometer, Fourier transform infrared spectra (FTIR) were recorded in the range (4000–400 cm^{-1}). As KBr disks, spectra were obtained. The electronic spectra of ligands and their complexes were calculated in DMSO solutions with a concentration of (10^{-3}-10^{-5} M) using a JASCO-V-650 UV-Visible Spectrophotometer. On a Bruker 500MHz SWISS TS AG, ^{1}H NMR spectra were recorded. an NOV AA (F.A.A) 350G atomic absorption spectrophotometer was used to determine the metal content of complexes. Jenway conductivity meter model 4070 was used to record conductivity measurements of the complexes at (25°C) for (10^{-3} mole L^{-1}) solution of the samples in DMSO.

RESULTE AND DISSCUTION

In this study, the chemical compounds (Schiff's base), (secondary amine) and (ligand salt) were prepared, as it included the preparation of a Schiff base from the reaction of the primary amine with 2-bromobenzaldhyde with the presence of methanol solvent, after the formation of a Schiff base that was dissolved in The solvents of ethanol and dichloromethane were then added $NaBH_4$ to give the product, which is the secondary amine, where the amine was dissolved, then carbon disulfide (CS_2) and the base (KOH) were added, which gave the ligand salt in a good proportion. The metal ratio is 1:1. In this reaction, the metal ion plays a large and prominent role in the self-preparation of metal complexes. The product gave two general formulas for the complexes, which are the tetrahedral shape and the octahedral shape as shown in (Scheme 1). The prepared organic compounds were diagnosed by mass spectrometry, spectrometry. Infrared, melting point, molar conductivity, nuclear magnetic resonance spectroscopy, and UV-Visible.

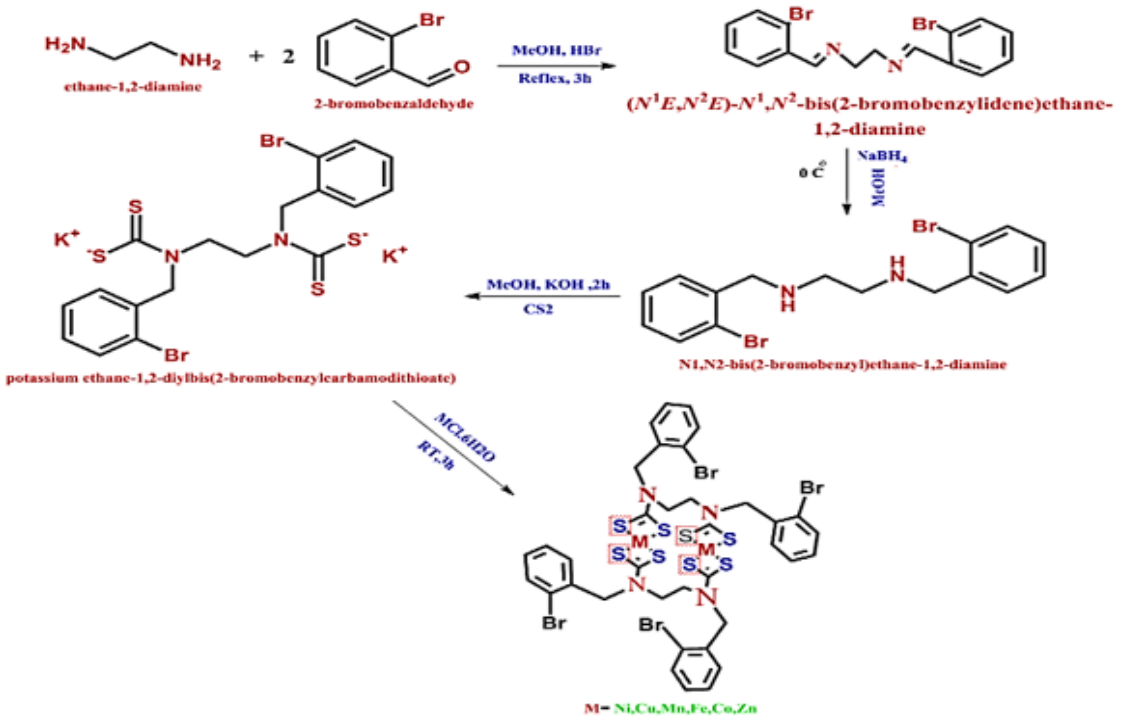

Scheme 1. Synthetic route of complexes (A) $[M(L)]_2$; where M = Mn(II), Fe(II), Co(II), Ni(II), Cu(II), Zn(II)

Table 1: Colour, yield, melting point, and molar conductivity of Complexes

Complexes	Weight of metal salt (g)	Weight of complex(g)	M.Wt	Yield (%)	Colour	m.p.^{o}C	ΣM(Ω cm^{-1} 2 mol) in DMSO
L	0.5	0.63	626.58	90	Off-white	100*	0.52
$[Mn(L)]_2$	0.4	0.99	1302.76	82	Dark brown	111*	0.39
$[Fe(L)]_2$	0.42	0.89	1304.58	74	Dark red	140*	0.98
$[Co(L)]_2$	0.23	0.36	1310.75	50	green	95*	0.3
$[Ni(L)]_2$	0.24	0.46	1382.34	65	green	255*	0.37
$[Cu(L)]_2$	0.11	0.19	1392.04	55	Dark green	103*	2.03
$[Zn(L)]_2$	0.11	0.29	1323.65	85	off-white	180*	0.56

FTIR spectra

Herein are presented the FTIR spectra of L (Fig. 1) and its complexes dipected in Table (2). Two bands at 1632-1585 cm^{-1} in the L FTIR spectrum referred to ν(C=N) and ν(C=C) of the pyridyl ring. The strong band in the range 1460-1500 cm^{-1} is explained by the ν(N-CS_2) stretching vibration. Compared to the unbound ligand at 1463 cm^{-1}, this band demonstrates an increase in the carbon-nitrogen double bond character. the bands at 1023 and 944 cm^{-1} in the ligand Anisobidentate chelation mechanism of the ligand was shown by these bands.[11,12] Also, the complexes of the first ligand appeared new absorption bundles linked to the ν(M-S) bond, namely ν(Mn-S) (439) cm^{-1}, ν(Fe-S) (439) cm^{-1}, As in ν(Co-S), (424) cm^{-1}, ν(Cu-S) (432) cm^{-1}, ν(Zn-S) (408) cm^{-1}[13] Table (2).

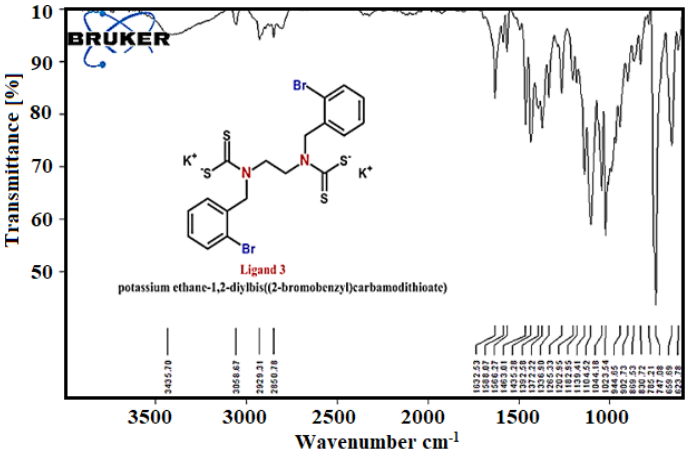

Fig. 1. FTIR Spectra of ligand. [L]

Table 2: FTIR spectral data (wave number) cm^{-1} of L3 and its complexes

Compound	νar(C=C)	ν(N-CS_2)	ν(C-N)	$\nu_{as,s}(CS_2)$	ν(M-S)
L	1566	1463	1265	1023, 944	_
$[Mn(L)_2]$	1512	1423	1342	10,02,860	439
$[Fe(L)]_2$	1566	1435	1346	10,22,983	439
$[Co(L)]_2$	1562	1438	1323	10,02,891	424
$[Ni(L)]_2$	1566	1485	1346	10,26,948	416
$[Cu(L)]_2$	1516	1423	1369	10,45,960	432
$[Zn(L)]_2$	1516	1419	1319	1026	408

Electronic_ spectra and magnetic moments

The UV-Vis spectra of the Mn^{+2} complex showed an absorption peak at (518) nm, (19305) cm^{-1}, which goes back to $^6A_{1g} \rightarrow {}^4T_{1g}(G)$, in which this transition is attributed to the tetrahedral[14,15] As for the Fe^{+2} complex, an absorption peak of (554) nm, (18050) cm^{-1} appeared, with an electronic transition of the d-d type, which belongs to the transition $^5E_2 \rightarrow {}^5T_2$, which is attributed to this transition to the tetrahedral shape[16,17]. For the Co^{+2} complex, a peak appeared at (641) nm, (15600) cm^{-1}, which is due to the transition $^4T_{1g}(F) \rightarrow {}^4T_{2g}(P)$, which is attributed to this transition to the tetrahedral shape[12].For the Ni^{+2} complex, the spectrum

shows two main peaks at(640) nm, (15625) cm^{-1} which refers to the transition $^1A1g \rightarrow {}^1A_{2g}$, which is attributed to this transition to the square planar shape[15]. For the Cu^{+2} complex, a peak at (658) nm, (975) cm^{-1} is due to the transition $^2B_{1g} \rightarrow {}^2A_{1g}$, which is attributed to this transition to the tetrahedral shape[15]. For the Zn^{+2} complex, a peak appeared at (425) nm, (23529) cm^{-1} which is C.T. The transition is attributed to the tetrahedral shape[18,19] see Table (3).

Table 3: UV-Vis Spectral data of L in DMSO solutions

Compound	Concen. mol/L	Band Positio n λnm	Wave number (cm^{-1})	Assignment	Suggested geometry
$[Mn(L)]_2$	1×10^{-5}	262	38167	Intra-ligand $\pi \rightarrow \pi^*$	Tetrahedral
		306	32679	$n \rightarrow \pi^*$	
		518	19305	$^6A_{1g}(F) \rightarrow {}^4T_{1g}(G)$	
$Fe(L)]_2$	1×10^{-5}	275	17391	Intra-ligand $\pi \rightarrow \pi^*$	Tetrahedral
		315	31746	$n \rightarrow \pi^*$	
	1×10^{-3}	554	18050	$^5E_2^{D}) \rightarrow {}^5T_2^{(D)}$	
$[Co(L)]_2$	1×10^{-5}	269	37174	Intra-ligand $\pi \rightarrow \pi^*$	Tetrahedral
		325	30769	$n \rightarrow \pi^*$	
		423	23640	C.T	
	1×10^{-3}	641	15600	$^4T_{1g}^{(F)} \rightarrow {}^4T_{2g}^{(P)}$	
$[Ni(L)]_2$	1×10^{-5}	259	38610	Intra-ligand $\pi \rightarrow \pi^*$	square planar
		394	25380	$n \rightarrow \pi^*$	
1×10^{-3}	640	15625	$^1A_{1g} \rightarrow {}^1A_{2g}$		
$[Cu(L)]_2$	1×10^{-5}	260	38461	Intra-ligand $\pi \rightarrow \pi^*$	Tetrahedral
		401	24937	$n \rightarrow \pi^*$	
	1×10^{-3}	658	15197	$^2B_{1g} \rightarrow {}^2A_{1g}$	
$[Zn(L)]_2$	1×10^{-5}	262	38167	Intra-ligand $\pi \rightarrow \pi^*$	Tetrahedral
	425	23529	C.T		

^{1}H NMR SPECTRUM

^{1}H NMR spectrum for ligand (L)

The structural formula of the prepared compound was confirmed using ^{1}H-NMR proton nuclear magnetic resonance spectroscopy and using the solvent [DMSO-d_6], which gave further evidence for the correctness of the product formation through the disappearance of the single signal at the region [δ = 4.6ppm] of a proton. The secondary amine group and the single sign appearing at the range [δ = 3.84ppm, (2H, s), CH_2 alip.], is due to (C6,6`-H), Belonging to the protons of the two symmetric aliphatic groups in the compound, and a single signal appeared at the range [δ = 4.24ppm, (2H, s) $CH_2$ benzyl], is due to (C5,5`-H), belonging to the two proton groups associated with the homologous aromatic ring in the compound, and the multiple signals of the aromatic ring protons at the range [δ = 7.89-8.21 ppm, (4H, m), Ar-H], is due to ($C_{1,1`,2,2`,3,3`,4,4`}$-H), which show a clear correspondence with the values in The scientific literature[20,21].

Table (4) shows the chemical displacement of the prepared compound diagnosed by the NMR spectrum measured in ppm. Shown in Figure (2).

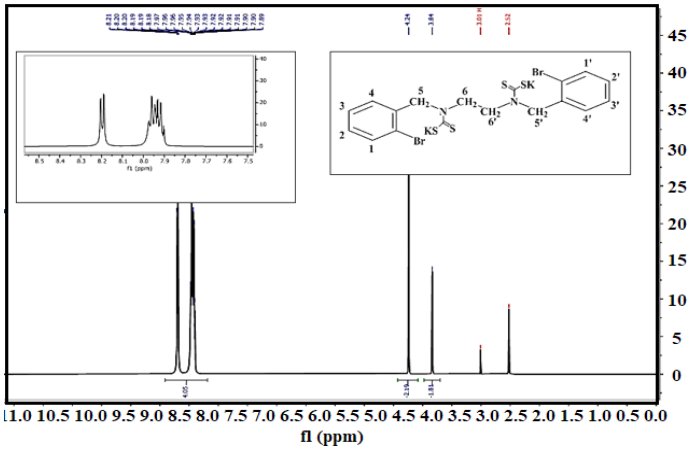

Fig. 2. ^{1}H NMR spectrum of in ligand L in DMSO-d_6

^{1}H NMR spectrum of $[Zn(L)]_2$

The structural formula of the prepared compound was confirmed using ^{1}H-NMR proton nuclear magnetic resonance spectroscopy and using the solvent [DMS0-d_6], which gave further evidence for the correctness of the product formation through the observed change in the locations of the chemical displacements of the protons and the increase in the number of protons it showed. The spectrum, showing a single signal at the range (δ = 3.76ppm, (4H, s), CH_2 alip.), is due to ($C_{6,6`}$-H) Belonging to the protons of the symmetric aliphatic groups in the compound, and a single signal at the range [$\delta$ = 4.68ppm, (4H, s) , $CH_2$ benzyl], is due to ($C_{5,5`}$-H), Belonging to the protons of the two groups associated with the symmetric aromatic ring in the compound, and the multiple signals of the aromatic ring protons at the range [δ = 7.81-8.42 ppm, (8H, m), Ar-H], is due to ($C_{1,1`,2,2`,3,3`,4,4`}$-H), which show a clear correspondence with the values in the literature Scientific[22,23]. Table (4) shows the chemical displacement of the prepared compound diagnosed by the NMR spectrum measured in ppm. shown in Figure (3).

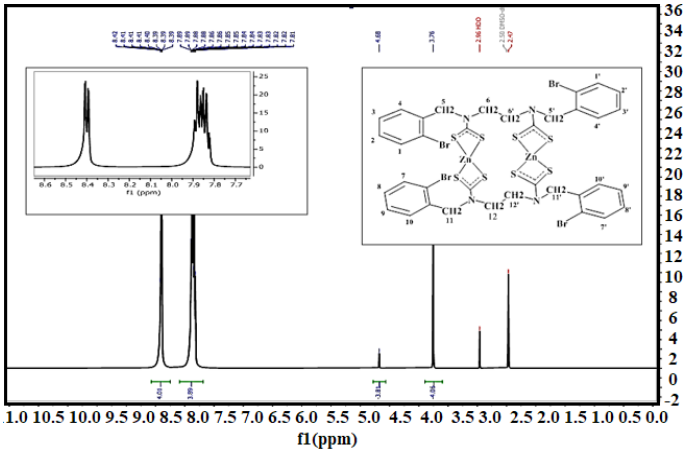

Fig. 3. ^{1}H NMR spectrum of $[Zn(L)]_2$ in DMSO-d^6

Table 4: ^{1}H-NMR data for ligand and Complex in DMSO-d_6

Compound	Functional group	δ = (ppm)
Free ligand L	($C_{6,6`}$-H)	3.84 (2H,s),
	($C_{5,5`}$-H)	4.24 (2H, s)
	($C_{1,1`,2,2`,3,3`,4,4`}$-H) aromatic ring	7.89-8.21 (4H, m)
	DMSO	2.51
	HDO	3.33
[Zn(L)] 2	($C_{6,6`}$-H)	3.76 (4H, s)
	($C_{5,5`}$-H)	4.68ppm, (4H, s)
	($C_{1,1`,2,2`,\ 3,3`,4,4`}$-H) aromatic ring	7.81 - 8.42 (8H, m)
	DMSO	2.51
	HDO	3.31

Mass spectrum

Mass spectrum of Schiff base

The electrospray (+) mass spectrum of Schiff base is presented in Fig. 4. A series of fragments related to ligand structure can be seen in the spectrum. the parent ion peak for the ligand at m/z = 394.95, which corresponds to (M) + (percent) for $C_{16}H_{14}Br_2N_2$; requires = 394.16, as well as other fragments, relative abundance, and fragmentation pattern shown in Table (5).

Mass spectrum of secondary amine

The electrospray (+) mass spectrum of secondary amine. is presented in Fig. 5. A series of fragments related to ligand structure can be seen in the spectrum. The ligand's parent ion peak is found at m/z = 395.2, which corresponds to (M)+ (percent) for $C_{16}H_{18}Br_2N_2$; requires = 398.14, as well as other fragments, their relative abundance, and fragmentation pattern are shown in Table (6).

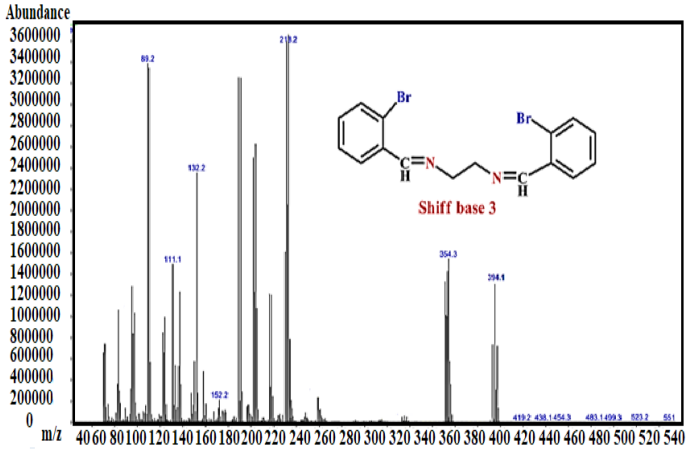

Fig. 4. The GC-EI (+) mass spectrum of Schiff base

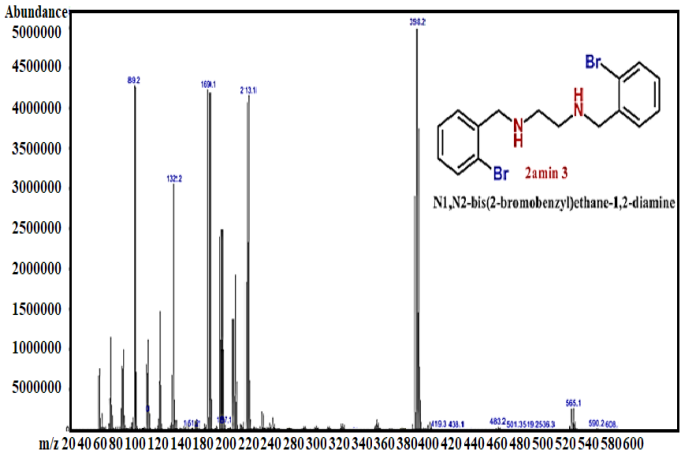

Fig. 5. The GC-EI (+) mass spectrum of secondary amine

Table 5: GC-Mass data of the Schiff base

Fragment	Mass/charge(m/z)
[M]=[$C_{16}H_{14}Br_2N_2$+H]	394.95
[$C_{13}H_{13}Br_2N_2$]$^+$	354.94
[[$C_8H_{10}BrN_2$]$^+$	213
[$C_4H_{10}BrN$]$^{\bullet+}$	152
[$C_9H_{12}N$]$^+$	134.1
[C7H12N]$^+$	111.1
[$C_4H_{13}N_2$]$^+$	89.16

Table 6: GC-Mass data of the secondary amine

Fragment	Mass/charge(m/z)
[M]=[$C_{16}H_{18}Br_2N_2$$^+$H]	395.2
[$C_9H_{11}BrN$]$^+$	213.1
[[C_7H_6Br]$^+$	169.1
[C_4H_4Br]$^+$	132.2
[$C_4H_{11}N_2$]$^-$	88.1

Mass spectrum of free ligand [L]

The electrospray (+) mass spectrum of KL is presented in Fig. 6. A series of fragments related to ligand structure can be seen in the spectrum. The ligand parent ion peak is found at m/z = 625.4, which corresponds to (M)+(percent) for $C_{18}H_{16}Br_2K_2N_2S_4$; requires = 626.58, as well as other fragments and their relative abundance and fragmentation pattern are shown in Table (7).

Table 7: GC-Mass data of the ligand KL

Fragment	Mass/charge (m/z)
[M]=[$C_{18}H_{16}Br_2K_2N_2S_4$ $^+$H]	625.4
[$C_{12}H_{13}BrKN_2S_3$]$^+$	400.2
[$C_{11}H_{14}BrN_2S_2$]$^+$	288.2
[$C_{15}H_{21}N_2S$]$^+$	262.1
[C3H7 Br N]$^+$	138.2
[$C_4H_{11}N_2$]$^\bullet$	89.2
[CH_3S]$^+$	50.1

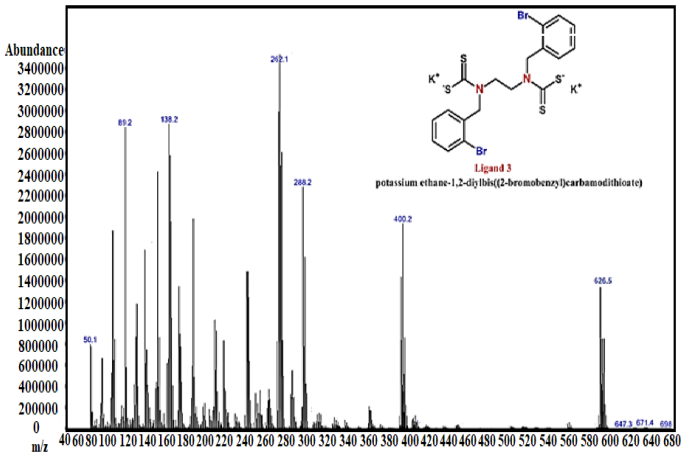

Fig. 6. The GC-EI (+) mass spectrum of L

Antibacterial activity

The results studied at concentrations of 50 mg/mL and one 100 mg/mL and compared with anti-inflammatory such as Ciprofloxacin and Levofloxacin standards showed: that ligand shows antimicrobial activity against *Escherichia coli (E. coli)* and *Staphylococcus aureus*. However, the free ligand showed higher antimicrobial activity against *Escherichia coli (E. coli)*, of the metal complexes compared with some of the measured antibiotics, see Table (8,9). Furthermore, the $[Cu(L)]_2$ complexes showed higher activity against *Staphylococcus aureus* compared to the free ligand at concentration (100,50) indicated that significant inhibitory activity was observed at concentration (100 mg/mL) for ($[Mn(L)]_2$, $[Fe(L)]_2$, $[Co(L)_2]$, $[Ni(L)]_2$, $[Zn(L)]_2$ compounds, while, $[Mn(L)]_2$, $[Fe(L)]_2$, $[Ni(L)]_2$, [and $[Zn(L)]_2$ at its concentration (50 mg/ml) showed moderate inhibiting activity among most bacteria[24,25].

Table 8: Results of an antibacterial study of complexes and prepared ligand

No	Complexes	Conc.mg/mL	*Staphylococcus aureus*	*Escherichia coli*
1	KL	50	20	27
		100	25	32
2	$[Mn(L)]_2$	50	12	11
		100	15	13
3	$[Fe(L)]_2$	50	12	10
		100	15	11
4	$[Co(L)]_2$	50	22	16
		100	23	18
5	$[Ni(L)]_2$	50	16	12
		100	22	17
6	$[Cu(L)]_2$	50	32	24
		100	32	25
7	$[Zn(L)]_2$	50	17	14
		100	25	16

Table 9: The inhibitory activity of a number of control factors (antibiotics) on the growth of a number of positive and negative bacteria

No	Complexes	Conc.mg/ml	*Staphylococcus aureus*	*Escherichia coli*
1	Ciprofloxacin	50	--	25
		100	--	26
2	Levofloxacin	50	--	25
		100	--	26

CONCLUSION

In this research, the free ligand and its interaction with ions of metallic elements were prepared and diagnosed and the complexes were given the stereoscopic shape through spectroscopic and analytical measurements that proved the formation of two types of shapes, the

tetrahedral shape and the square planar around the center of the metal. The complexes' biological activity was tested on a variety of bacterial strains. Pathogens such as *Escherichia coli (E. coli)* and *Staphylococcus aureus* were particularly vulnerable to the complexes. After examining the in vitro effect of metal complexes on experimental animals and clinical trials, the current study suggested that complexes will be employed as promising candidates for further biological evaluation.

ACKNOLEGMENT

We want to express my sincere gratitude to the Departments of Chemistry and Biology at University of Anbar for its invaluable support and resources throughout our research.

Conflict of interest

The author declare that we have no conflict of interest.

RERERENCES

1. Yousif, E.I.; Ahmed, R.M.; Hasan, H.A.; Al-Fahdawi, A.S.; Al-Jeboori, M.J., *Iranian Journal of Science and Technology, Transactions A: Science.*, **2017**, *41*, 103-109.
2. Breijyeh, Z.; Karaman, R.; *Antibiotics (Basel, Switzerland).*, **2023**,*12*(3), 628.
3. Bakheit, A.H.; Al-Salahi, R,; Ghabbour, H. A.; Ali, E.A.; AlRuqi, O. S.; Mostafa, G. A .E., *Crystals.*, **2023**, *13*(7), 1088.
4. Alsalihi, I.I.; Al-khafaji, Y.F,; Al-fahdawi, A.S.; Atiyah E M., *Bulletin of the Chemical Society of Ethiopia.*, **2022**, *36*(4), 791-799.
5. Liu, R.; Cui, J.; Ding, T.; Liu, Y.; Liang, H., *Molecules (Basel, Switzerland).*, **2022**, *27*(23), 8393.
6. Juliet, A.A.; Hameed, A.T.; Ali, F.F., *HIV Nursing.*, **2022**, *22*(2), 1631-4.
7. Abdulqader, I. A.; Al-Fahdawi , A.S.; fadhel Ali, F.; Journal of Survey in Fisheries Sciences. 2023, 10(3S):2890-905.
8. Saleh, S.; Al-Timari, U.; Al-Fahdawi , A.; El-Khatatneh, N.A.; Mahendra, M.; Al-Ghorbani, M., *Oriental J. Chem.*, **2017**, *33*(6), 2713-9.
9. Yan, Y.; Li, X.; Zhang, C.; Lv, L.; Gao, B.; Li, M., *Antibiotics (Basel, Switzerland).*, **2021**, *10*(3), 318.
10. Muteeb, G.; Rehman, M.T.; Shahwan, M.; Aatif, M., *Pharmaceuticals.*, **2023**, *16*(11), 1615.
11. Ghoto, S.A.; Khuhawar, M.Y.; Jahangir, T.M., *Analytical Sciences.*, **2019**, *35*(6), 631-7.
12. Al-Obeidi, F.Z.; Al-Fahdawi , A.S.; Al-Jeboori, M.J., *J. Global Pharma Technol.*, **2018**, *10*(03), 699-710.
13. Abdullah, S.A.; Othman, E.A.; Al-Fahdawi, A.S., *Samarra Journal of Pure and Applied Science.*, **2020**, *2*(3).
14. Al-Mohammadi, N.A.; Al-Fahdawi , A.S.; Al-Janabi, S.S.; *Iraqi J. of Science.*, **2021**, *30*, 1-5.
15. Al-fahdawi, A.S.; Al-Sorchee, S.M.; Saleh, S.E.; Saleh, M.M., *Egyptian Journal of Chemistry.*, **2021**, *64*(6), 2879–2888.
16. Salih, B.D.; Dalaf, A.H.; Alheety, M.A.; Rashed, W.M.; Abdullah, I.Q., *Materials Today: Proceedings.*, **2021**, *1*(43), 869-74.
17. Al-Fahdawi, A. S.; Herman, P.; Al- Jeboori, M. J., *Asian J. of Green Chem.,* **2025**, *9*(1), 32-42.
18. Andrew, F.P.; Ajibade, P.A., *International Journal of Electrochemical Science.*, **2019**, *1;14*(8), 7062-75.
19. Al-fahdawi, A.S.; Mohamed, S.K.; Potgeiter, H; Alfutimie, A., *Bulletin of the Chemical Society of Ethiopia.*, **2024**, *38*(6), 1583-93
20. Yousif, E.I.; Hasan, H.A., *Ibn AL-Haitham Journal For Pure and Applied Science.*, **2017,** *11;30*(1), 73-87.
21. Sultan, J.S.; Alsalihi, E.I.; Al-Fahdawi, A.S.; Jabar, A., *Egyptian Journal of Chemistry.*, **2020**, *63*(1), 325–335
22. Hussain, S.; Zahid, Z.; Shahid, M,; Abid M.A., *Arabian Journal for Science and Engineering.*, **2019**, *1;44*, 6423-34.
23. Al-Sorchee, S.M.; Ismail, T.F.; Mohammed, I.M.; Al-fahdawi, A.S., *Biochemical and Cellular Archives.*, **2020**, *20*(1), 373–382
24. Al-Obaidy, G.S.; Al-Dulymi, Hk.Hk.; Abed, M.A., *Sciences.*, **2024**, *22*(2), 1082-93.
25. Singh, R.V.; Dwivedi, R.; Joshi, S.C., *Transition Metal Chemistry.*, **2004,** *29*, 70-4.